Structural and Dielectric Properties of Strontium Hexaferrite Powder Synthesized in Presence of Crown Flowers Extract

Chetna Chauhan[1*], Tanuj Gupta[2] and Rajshree Jotania[3]

[1,2]*Institue of Technology, Nirma University, Ahmedabad – 382 481. Gujarat.*

[3]*Department of Physics, University School of Sciences, Gujarat University, Navrangpura, Ahmedabad – 380 009. Gujarat.*

*chetna.chauhan@nirmauni.ac.in

Abstract:

Strontium hexaferrite ($SrFe_{12}O_{19}$) powder was synthesized in presence of Calotropis Gigantea (crown) flowers extract. The stoichiometric proportion of strontium nitrate and ferric nitrate were added one by one in crown flowers extract and heated at 650º C for 6 hrs to obtain Strontium hexaferrite powder. Structural properties of calcined powder were investigated using FTIR and XRD analysis. FTIR study reveals the formation of ferrite phase. XRD analysis shows presence of M and α-Fe_2O_3 phases. The real and imaginary part of dielectric constant is measured at room temperature between 20 Hz to 2 MHz frequency. The dielectric behaviour of prepared strontium hexaferrite powder is described using Maxwell-Wagner bilayer model and Koop's theory.

Keywords

Strontium hexaferrite, Calotropis Gigantea flowers extract, Structural and dielectric properties.

1. Introduction

The M type strontium hexaferrites are suitable magnetic materials for permanent magnets, due to their distinct magnetic properties like high Curie temperature, large value of magnetocrystalline anisotropy constant, high permeability, excellent chemical stability and corrosion resistance [1-4]. The M type hexagonal ferrites possess magnetoplumbite crystal structure and can be considered as a superposition of spinel and hexagonal layers made up of $Fe_6O_8^{+2}$ and $MeFe_6O_{11}^{-2}$ (where Me represents bivalent metal ions like Ba, Sr, Pb or Ca) . The M type of strontium hexaferrite has 24 Fe^{+3} ions per unit cell and they are arranged among five different interstitial sites: three on octahedral sites 12k, 2a and $4f_2$, one at tetrahedral site $4f_1$ and rest of one at trigonalbipyramidal site 2b. The three octahedral sites have parallel spins; whereas the tetrahedral and bipyramidal sites have anti-parallel spins.

Hexaferrites can be prepared by variety of physical and chemical methods. Several methods like co precipitation [5], microemulsion [6], hydrothermal synthesis [7] sol gel [8,9], salt-melt [10], ion exchange [11], citrate synthesis [12], glass crystallization [13, 14] have been proposed to prepare hexaferrites. In the current study, we report the structural and dielectric properties of $SrFe_{12}O_{19}$ powder; synthesized using Calotropis Gigantea flowers extract and heated at 650º C for 6 hrs.

2. Experimental Procedure

The fresh flowers of Calotropis Gigantea were collected from the outside of Nirma University campus, Ahmedabad and then washed with normal water followed by double distilled water. 30 g of Crown flowers were cut into fine pieces and then boiled in 100 ml de-ionized water for 15 min. and cooled to room temperature. The mixture was filtered and used as flowers extract. Stochiometric proportion of strontium nitrate [$Sr(NO_3)_2$, Sigma- Aldrich, $\geq$ 9.995 %] and iron (III) nitrate nonahydrate [$Fe(NO_3)_3.9H_2O$, Sigma-Aldrich, $\geq$ 98 %] were taken and dissolved one by one in to flowers extract and mixture was rigorously stirred for one hour at room temperature. The homogenous mixture so obtained was kept in oil bath at 100º C under continuous stirring till the brownish color dried precursors were obtained. The dried precursors were preheated at 500º C for 4 hrs and then calcined in presence of air at 650º C for 6 hrs inside a muffle furnace to obtain $SrFe_{12}O_{19}$ powder.

3. Results and Discussion

3.1 FTIR Analysis
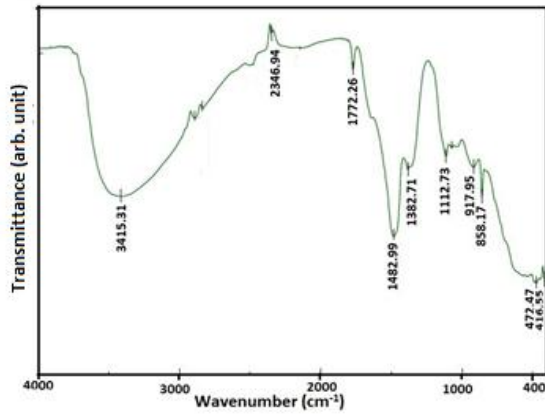
Figure 1. FTIR spectrum of SrFe$_{12}$O$_{19}$ powder synthesized in presence of Crown flowers extract and heated at 650º C for 6 hrs.

Figure 1 shows the FTIR spectrum of SrFe$_{12}$O$_{19}$ powder recorded between the wavenumber 4000 cm^{-1} to 400 cm^{-1}. The first absorption band near 3400 cm^{-1} represents the presence of O-H vibrations [15] and other strong absorption band at 1400 cm^{-1} corresponds to the presence of small amount of residual carbon [16]. The characteristic absorption bands of the ferrite phase (Fe-O stretching vibrations) are found between 600 to 400 cm^{-1} [17].

3.2 XRD Analysis
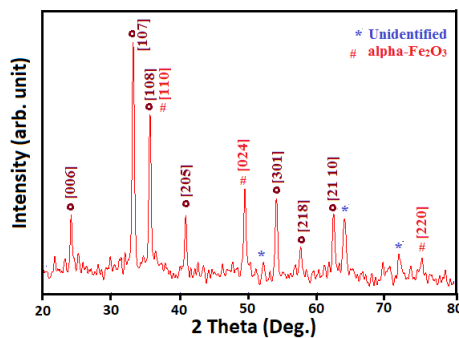
Figure 2. X-ray diffraction pattern of SrFe$_{12}$O$_{19}$ powder synthesized in presence of Crown flowers extract and heated at 650º C for 6 hrs.

Bruker D Z Phaser diffractometer (PW 1830, Cu- Kα radiation- λ=1.5405 Å) with the scan rate of 2º /min was used to study structural properties. Figure 2 shows the XRD pattern of SrFe$_{12}$O$_{19}$ powder recorded at room temperature. The obtained peaks in XRD patterns were identified using Powder-X software. The diffraction peaks corresponding to the planes [006], [107], [108], [205], [301], [218], [21 10] matched with M-type hexagonal crystal structure (PDF # 801198, a = 5.883 Å, c = 23.039 Å, V_{cell} = 690.64 Å^3), while the diffraction peaks corresponding to the planes [110], [024], [220] matched with α-Fe$_2$O$_3$ crystal structure (CAS registry No. 1309-37-1).

Three peaks at 2θ ~ 52.191°, 64.015°, 71.920° remain unidentified.

Equations (1) and (2) were used to calculate the cell parameters (a, c) and unit cell volume (V_{cell}) respectively.

For hexagonal crystal structure a = b ≠ c and $\alpha = \beta$ = 90° and γ = 120°

$$\frac{1}{d_{hkl}} = \frac{4}{3}\left(\frac{h^2}{a^2} + \frac{hk}{a^2} + \frac{k^2}{a^2}\right) + \frac{l^2}{c^2} \qquad (1)$$

Where d$_{hkl}$ is d-separation of the lines in XRD pattern and h,k,l are Miller indices.

$$V_{cell} = \frac{\sqrt{3}}{2} a^2 c \qquad (2)$$

Debye Scherrer's equation (Eq.3) [18] was used to calculate the average crystalline size (D_{xrd}) of SrFe$_{12}$O$_{19}$ powder. The strongest Bragg's peak (111) was considered.

$$D_{XRD} = 0.9\frac{\lambda}{\beta\cos\theta} \qquad (3)$$

Where
λ - wavelenght of X-rays (1.5405 Å) ;
θ - Bragg's angle of diffraction;
β - the line broadning at half of the maximum intensity (FWHM), after substracting the instrumental line broadening, in radians.

Lattice parameters, unit cell volume, ratio *(c/a)* and crystalline size of SrFe$_{12}$O$_{19}$ powder are listed in Table 1.

Table 1. Lattice parameters (a, c), unit cell volume (V_{cell}) and crystallite size (D_{XRD}) of SrFe$_{12}$O$_{19}$ powder synthesized in presence of Crown flowers extract and heated at 650º C for 6 hrs.

SrFe$_{12}$O$_{19}$ powder	
Lattice parameters	a (Å) = 5.883
	c (Å) = 23.039
(c/a) ratio	3.916
Cell Volume V$_{cell}$ (Å^3)	690.64
Crystallite Size D$_{XRD}$ (nm)	20.67 ± 1.03

3.3 Dielectric Measurements
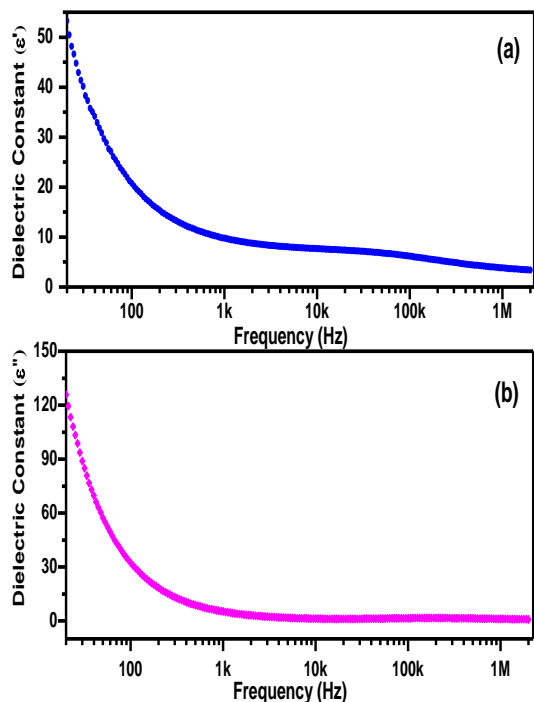
Figure 3(a,b). Frequency dependent real dielectric constant (ε') and imaginary dielectric constant (ε'') of SrFe$_{12}$O$_{19}$ powder synthesized in presence of Crown flowers extract and heated at 650º C for 6 hrs.

The dielectric measurements of SrFe$_{12}$O$_{19}$ powder synthesized in presence of Crown flowers extract and heated at 650º C for 6 hrs were carried out at room temperature on Agilent Precision LCR meter (Model No. E4980A) over the frequency range 20 Hz to 2 MHz. Figure 3 (a, b) shows change in real and imaginary part of dielectric constant with frequency at room temperature. The larger values of dielectric constant are observed at lower frequencies. Figure 3 (a, b) reveals that both real as well as imaginary part of dielectric constants decrease with the increase of frequency and remain almost constant at higher frequencies. Larger values of dielectric constant below 100 HZ frequency are due to presence of inhomogeneity in the sample arising from grain boundary defects, dislocations, voids, Fe^{+2} ions, etc. [19]. Reduction in dielectric constant at lower frequencies can be explained by Koop's and Maxwell-Wagner interfacial theory [20]. As per this theory; the dielectric material consists of a conducting layer (grains) seperated by the non comducting layer (grain boundaries) The direct contact of dielectric mateirals with atmosphere results in the formation of grain boundaries during the heating process [21]. The charge carriers move toward the grain boundaries by the hopping process during the conduction phenomena. High resistance at grain boundaries results in the accumulation of charge carriers near the grain boundaries and produces the polarization of the

material, which increases the dielctric constant [22]. At higher frequecy, lower value of resistance decreases the polarization, which leads to the decrease in dielectric constant.
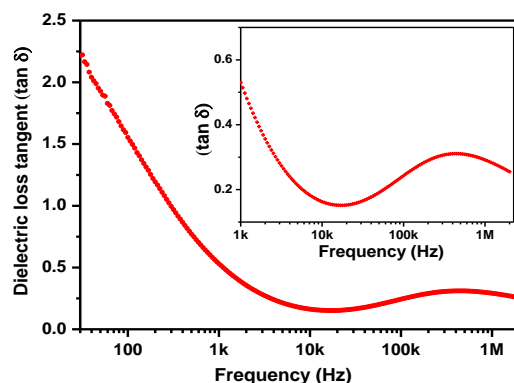
Figure 4. Variation of dielectric loss tangent (tan δ) with frequency of SrFe$_{12}$O$_{19}$ powder synthesized in with Crown flowers extract and heated at 650º C for 6 hrs.

The alternating field at higher frequencies cannot effect the hopping phenomena because of the small relaxation time. These resist the flow of charge carriers approaching towards grain boundaries and decrease the polarization effect. The dielectric loss tangent *(tan δ)* values were calculated using the relation [23].

$$\varepsilon'' = \varepsilon'(\tan\delta) \qquad (4)$$

Where (ε') and (ε'') are real and imaginary part of dielectric constant. It is clear from Figure 4 that (tan δ) is observed to be decrasing with increasing applied frequency. At higher frequencies, polarization lags behind the applied electric field resulting in the piling up of charge carriers near the grain boundaries. The increase in charge carriers near the grian boundaries resist the movement of dipoles, which decreases the dielectric loss tangent at higher frequencies.
The dielectric loss tangent for hexaferrite depends on variety of factors like stochiometry, structure, number of charge carriers etc. which again depends on the method of preparation and calcination temperature of the mateirals [24]. The materials with higher value of conductance exhibits higher dielectric losses and vice versa [25]. In present case, the dielectric loss tangent is observed to be decreasing at lower frequencies and then it increases (Figure 4) between frequency ranges of 30 kHz to 500 kHz. The broadening in the dissipation curve with the increase of frequency is due to the orientation of the dipoles with the alternating field as reported earlier [26]
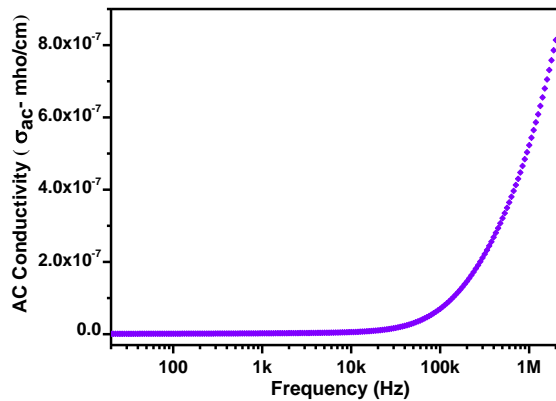
Figure 5. AC conductivity (σ_{ac}) variation with frequency of SrFe$_{12}$O$_{19}$ powder synthesized in presence of Crown flowers extract and heated at 650º C for 6 hrs.

Variation of Ac conductivity with frequency range of 20 Hz to 2 MHz is shown in Figure 5. The AC conductivity was calculated using the formula (5)

$$\sigma_{ac} = \omega\varepsilon_0\varepsilon'(\tan\delta) \qquad\qquad (5)$$

Where (ω) is angular frequency and ε_0 is permittivity in free space.

The increase in the value of AC conductivity is observed with the increase in externally applied frequency. There is sudden increase in the value of AC conductivity is observed above frequency > 100 kHz. As discussed in the dielectric constant characteristics the grains boundaries are more effective than grains at lower frequencies. It means that the conduction mechanisms are mainly controlled by the volume of grain boundaries. The motion of charge carries is affected by the grain boundaries in lower frequency region due to the low conductivity. Due to the higher resitance of grain boundaries, the grain boundareis act as a barriers to the conduction of material. An increase in the frequency, inceases the hopping of electrons therby increasing the conduction mechanism.

4. Conclusions

Strontium hexaferrite (SrFe$_{12}$O$_{19}$) powder has been sucessfully synthesized in presence of Crown flowers extract. The powder heated at 650º C for 6 hrs shows the presence of M and α- Fe$_2$O$_3$ phases in XRD analysis, FTIR study also reveals the formation of ferrite phase. The frequency dependent dielectric constants were observed to be decreasing with the increase in frequency; this behavior is explained by Maxwell- Wagner bilayer model and Koop's theory. The dielectric relaxation is observed and the broadening in the dissipation curve with the increase

of frequency is due to the orientation of the dipoles with an applied alternating field.

5. Acknowledgement

References

[1] Pullar, R. C., "Hexagonal ferrites: A review of the synthesis, properties and applications of hexaferrite ceramics", *Progress in Materials science*, 57, 2012, pp. 1191-1334

[2] Shinde, S. R., Lofland, S. E., Ganpule, C. S., Bhagat,S. M., Bhagat, S. B., Ogle, S. B., Ramesh, R., and Venkatesan, T., "Improvement in spin-wave resonance characteristics of epitaxial barium-ferrite thin films by using an aluminum-doped strontium-ferrite buffer layer", *Applied Physics Letters*, 74, 4, 1999, pp. 594.

[3] Chen, N., Yang, K., and Gu, M. Y., "Microwave absorption properties of La-substituted M-type strontium ferrites", *Journal of Alloys and Compounds*, 490, 1-2, 2010, pp. 609-612.

[4] Dho, J., Lee, E. K., Park, J. Y., and Hur, N. H., "Effects of the grain boundary on the coercivity of barium ferrite BaFe$_{12}$O$_{19}$," *Journal of Magnetism and Magnetic Materials,* 285, 1-2, 2005, pp. 164-168.

[4] Rai, B. K., Mishra, S. R., Nguyen, V. V., and Liu, J. P., *Journal of Alloys and Compounds*, "Synthesis and Characterization of high coercivity rare-earth ion doped Sr$_{0.9}$RE$_{0.1}$Fe$_{10}$Al$_2$O$_{19}$," 550, 2013, pp. 198-203.

[5] Zhong, W., Ding, W. P., Zhang, N., Hong, J., Yan, Q., and Du, Y., "Key step in synthesis of ultrafine BaFe$_{12}$O$_{19}$ by sol-gel technique" *Journal of Magnetism and Magnetic Materials,* 168 (1997) pp. 196-202.

[6] Drmota, A., Drofenik, M., and Znidarsic, A., "Synthesis and characterization of nano-crystalline strontium hexaferrite using the co-precipitation and microemulsion methods with nitrate precursors," *Ceramics International*, 38, 2, 2012, pp. 973-979.

[7] Kumazawa, H., Maedaand, Y., and Sada E., "Further Consideration of Hydrothermal synthesis of barium ferrite fine particles", *Journal of Materials Science Letter,* 14, 1995, pp. 68-70.

[8] Martinez Garcia, R., Bilovol, V., and Socolovsky, L. M., "Effect of the heat treatment conditions on the synthesis of Sr-hexaferrite," *Physica B-Condensed Matter,* 407, 16,

2011, pp. 3109-3112.

[9] Pullar, R. C., Appleton, S. G., and Bhattacharya, A. K., "The manufacture, characterisation and microwave properties of aligned M ferrite fibres," *Journal of Magnetism and Magnetic Materials,* 186, 1998, pp. 326-332.

[10] Arendt R. H., Van Buren C. E., US pat 3810937; 1974.

[11] Kagotani, T., Takamura H., Okada M., and Homma M., "Preparation and Magnetic properties of M type ferrite from β – ferrite single crystal by ion exchange and Se vapor annealing," In:Ferrites, proc. ICF6, Tokyo and Kyoto, 1992, pp.1137-1140.

[12] Sankaranarayan V.K.S, Pankhurst Q.A., Dickson D.P.E., and Jhonson C.E., "An Investigation of particle size effects in ultrafine barium ferrite," *Journal of Magnetism and Magnetic Materials,* 125, 1993, pp. 199-208.

[13] Sato H., Umeda T., "Structures and Magnetic Properties of rapidly solidified strontium and barium ferrites," In:Ferrites, proc. ICF6, Tokyo and Kyoto, 1992, pp.1122- 1125.

[14] Kurisu S., Kubo O., "Barium Ferrite crystallization process and their effects on particle properties in the glass crystallization method," In:Ferrites, proc. ICF6, Tokyo and Kyoto, 1992, pp.1398-1401

[15] Skoog, D. A., *Principles of Instrumental Analysis*, Saunders Golden Sunburst Series, 1985.

[16] Duo, M., Bruece, E. G., and Manuel, A. Q., "Ferroelectric Properties and Polarization Switching Kinetic of Poly (vinylidene fluoride-trifluoroethylene) Copolymer," *Ferroelectrics – Physical Effects*, In Tech, Chapter 4, 2011.

[17] Zhao, W. Y., Wei, P., Cheng, H. B., Tang, X. F., and Zhang, Q. J., *Journal of American Ceramic Society*, 7, 90, 2007, pp. 2095-2103.

[18] Kingery, W. D., Bowen, H. K., and Uhlmann. D. R., *Introduction to Ceramics*, 2nd Edition, Wiley, New York, 1976.

[19] Shrideshmukh, L., Kumar, K. K., Laxman, S. B., Krishna A. R., and Sathaiah, G., "Dielectric Properties and Electrical Conduction in Yttrium Iron Garnet (YIG)," *Bulletin of Materials Science,* 21, 3, 1998, pp. 219-226.

[20] Kao, K. C., *Dielectric Phenomena in Solids*. Elsevier, Los Angeles, Chap 2, pp. 51, 2004.

[21] Reddy, P. V. and Rao, T. S., "Dielectric Behaviour of Mixed Li-Ni Ferrites at Low Frequencies," *Journal of the Less Common Metals*, 86, 1982, pp.255-261.

[22] Iqbal, M. J. and Farooq, S., "Enhancement of Electrical Resistivity of $Sr_{0.5}Ba_{0.5}Fe_{12}O_{19}$ Nanomaterials by Doping with Lanthanum and Nickel," *Materials Chemistry and Physics*, 118, 2009, pp. 308-313.

[23] Gul, I. H., and Maqsood, A., "Influence of Zn-Zr ions on Physical and magnetic Properties of Co-precipitated Cobalt Ferrite Nanoparticles," *Journal of Magnetism and Magnetic Materials,* 316, 2007, pp. 13-18.

[24] Auwal, I. A., Ünal, B., Güngüneş, H., Shirsath, Sagar E., and Baykal A.,"Dielectric Properties ,cationic distribution calculation and hyperfine interactions of La^{+3} and Bi^{+3} doped strontium hexaferrites", *Ceramics International*, 42, 2016, pp. 9100-9115.

[25] Meena, R. S., Bharracharya, S., and Chatterjee, R., "Complex permittivity, permeability and wide-band microwave absorbing property of La^{+3} substituted U-type hexaferrite," *Journal of Magnetism and Magnetic Materials,* 322, 2010, pp. 1923-1928.

[26] Murthy, V. R. K. and Sobhanadri, J., "Dielectric properties of some nickel–zinc ferrites at radio frequency" *Physica Status Solidi A,* 36, K133–K135, 1976.